nature nanotechnology

LETTERS

PUBLISHED ONLINE: 6 APRIL 2009 | DOI: 10.1038/NNANO.2009.71

Tunable few-electron double quantum dots and Klein tunnelling in ultraclean carbon nanotubes

G. A. Steele*, G. Gotz and L. P. Kouwenhoven

Quantum dots defined in carbon nanotubes are a platform for both basic scientific studies[1–5] and research into new device applications[6]. In particular, they have unique properties that make them attractive for studying the coherent properties of single-electron spins[7–11]. To perform such experiments it is necessary to confine a single electron in a quantum dot with highly tunable barriers[1], but disorder has prevented tunable nanotube-based quantum-dot devices from reaching the single-electron regime[2–5]. Here, we use local gate voltages applied to an ultraclean suspended nanotube to confine a single electron in both a single quantum dot and, for the first time, in a tunable double quantum dot. This tunability is limited by a novel type of tunnelling that is analogous to the tunnelling in the Klein paradox of relativistic quantum mechanics.

Single spins in carbon nanotube quantum dots are expected to be very stable against both relaxation and decoherence[11]. Nuclear spins, the principal source of spin decoherence[7,8] in GaAs, can be completely eliminated and, furthermore, a strong spin–orbit interaction recently discovered in carbon nanotubes[9] allows all-electrical spin manipulation[10,11], while preserving long spin-relaxation and decoherence times[11]. Electron spins in carbon nanotube quantum dots are therefore attractive for implementation of a quantum bit (qubit) based on spin for applications in quantum-information processing[6]. In double quantum dot systems, precise control of the tunnel coupling between the two quantum dots, and between the quantum dots and the leads attached to them, is critically important for spin readout schemes[1,12,13], and also to prevent loss of spin and phase information through exchange of an electron with the leads.

Double quantum dots can also be used to explore novel quantum tunnelling phenomena. In Klein tunnelling[14–16], for example, an electron tunnels with a high probability through a potential energy barrier it would not normally tunnel through, when the height of the barrier is made comparable to twice the rest mass of the electron. It is not feasible to create such a barrier for free electrons due to the enormous electric fields required, but the low effective rest mass of the electrons in small-bandgap nanotubes makes the observation of such Klein tunnelling in nanotube devices possible[16].

By depositing metallic gates isolated by a dielectric layer on top of a nanotube, several groups have demonstrated tunable double quantum dots in nanotubes lying on a substrate[2–5]. These are tunable in the sense that the height and width of energy barriers between dots can be controlled by the gate. A disadvantage of this technique is that nanotubes in these devices suffer from significant disorder induced by the substrate and by the chemical processing required to fabricate the device. As the electron density is reduced, this random potential dominates and breaks the nanotube segment into multiple disorder-induced 'intrinsic' quantum dots before reaching the few-electron regime.

Wet etching of the device after fabrication to remove the substrate-induced disorder has been used previously to obtain single-electron quantum dots in carbon nanotubes[17,18], although experience has shown that the yield of such devices is quite low. Recently, a new fabrication method has been developed for producing ultraclean quantum dots in suspended carbon nanotubes with a high yield in which all chemical processing is done before nanotube growth[19]. Studying single quantum dots in these devices has uncovered new carbon nanotube physics, including a strong spin–orbit interaction due to the nanotube curvature[9] and evidence of Wigner crystallization of electrons at low density[20]. Although devices fabricated in this way are extremely clean, they have some significant limitations. In particular, the confinement is produced only by Schottky barriers, which cannot be easily tuned *in situ*. Furthermore it has not been possible to create a tunable double quantum dot in these ultraclean devices due to an insufficient number of local gates.

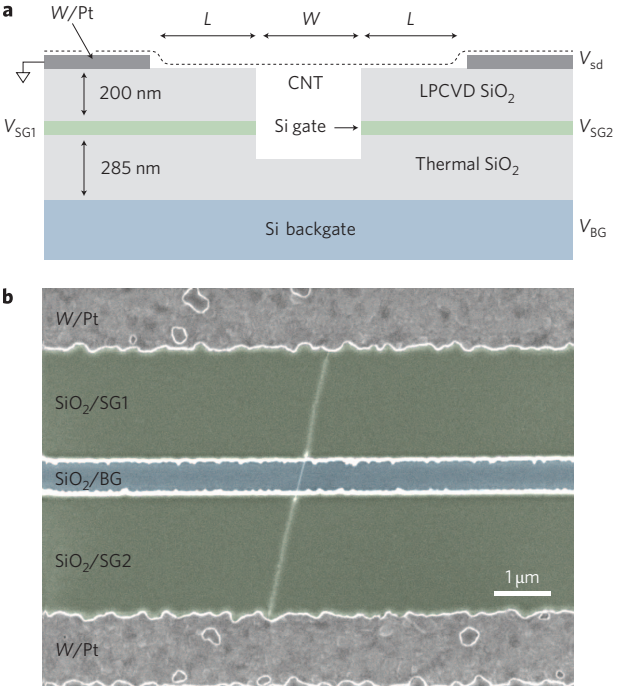

Figure 1 | Integrating local gates with ultraclean carbon nanotubes. **a**, Schematic of the device. A predefined trench is etched to create two splitgates from a 50-nm-thick n^{++} polysilicon gate layer (green) between two silicon oxide layers (grey). A platinum metal layer is deposited to act as source and drain contacts, and a nanotube is then grown from a patterned catalyst. Device D1 has dimensions $L = 1.5$ μm and $W = 300$ nm, and D2 has $L = 300$ nm and $W = 500$ nm. **b**, In a subset of devices, a single nanotube bridges the trench, contacting the metal source and drain electrodes (SEM image coloured for clarity). The micrograph shows an example of a device with the same dimensions as device D1.

Kavli Institute of NanoScience, Delft University of Technology, PO Box 5046, 2600 GA, Delft, The Netherlands. *e-mail: G.A.Steele@tudelft.nl

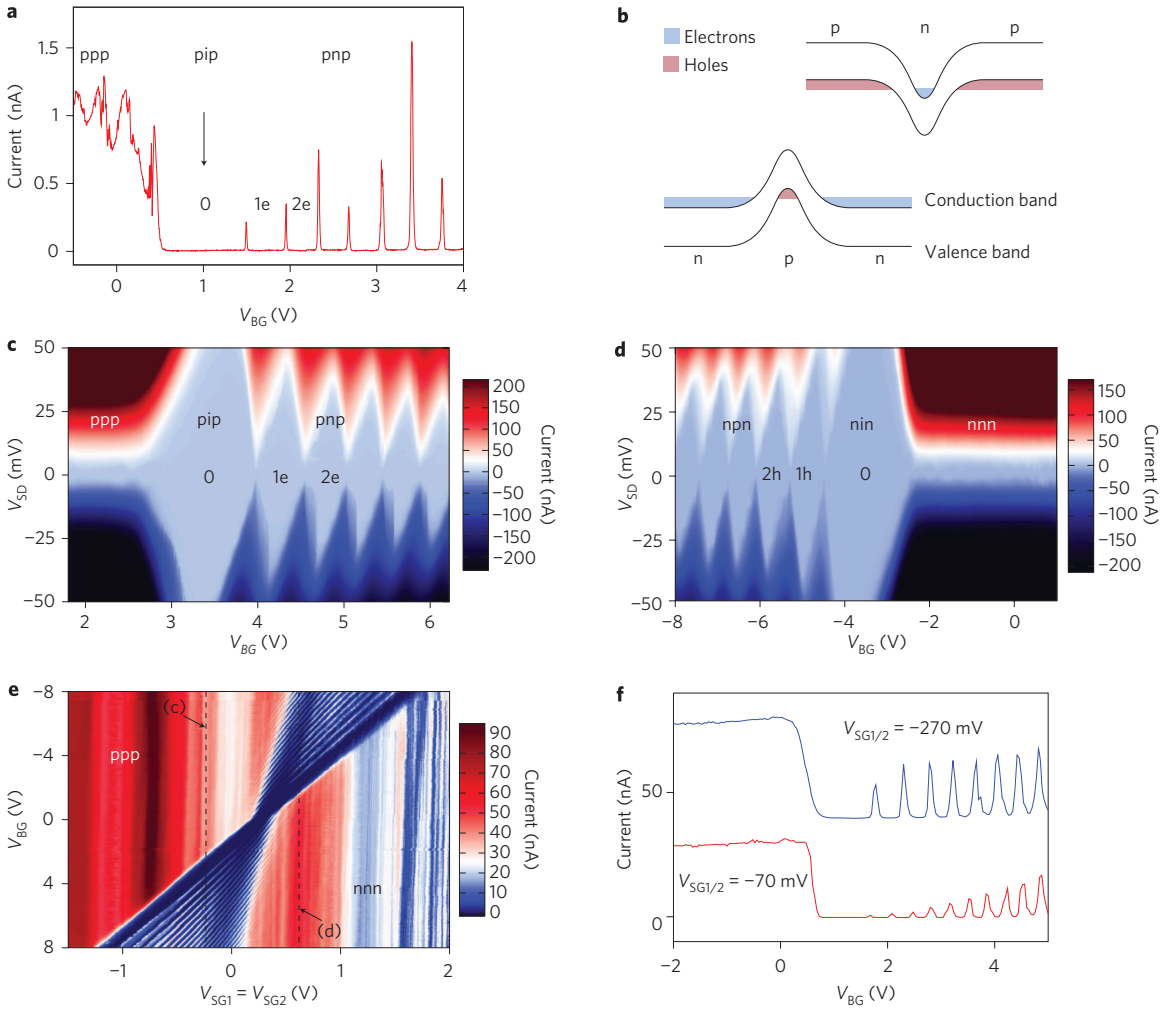

Figure 2 | Gate defined single-electron and single-hole quantum dots. a, Coulomb peaks of a pnp quantum dot in device D1 taken at a $V_{SG1} = V_{SG2} = -50$ mV and $V_{SD} = 1$ mV. The splitgates are used to dope the nanotube source and drain leads with holes. As V_{BG} is swept from negative to positive voltages, the suspended segment is depleted giving a pip configuration, followed by a pnp configuration as single electrons are filled in an n-type quantum dot. **b**, Energy diagrams showing pnp and npn quantum dots formed by p-n junction confinement. **c**, Stability diagram of the pnp dot: the charging energy of the first electron $E_c^{1e} \approx 40$ meV is remarkably large due to the weak capacitive coupling of the suspended segment to the gates and the metal source drain layers. **d**, The potential landscape in the device can be completely controlled by the gate voltages: by reversing the gate voltages, single holes are confined in a npn configuration. **e**, A two-dimensional plot showing backgate sweeps at different splitgate voltages and $V_{SD} = 10$ mV. The two splitgates are set to the same voltage. The stability diagrams in **c** and **d** are taken at $V_{SG1/2}$ values indicated by the dashed lines. (Resonances from residual disorder in the long nanotube leads can be seen as oscillations as a function of $V_{SG1/2}$ in the ppp and nnn configurations.) **f**, Using the splitgates, we can tune the width of the p-n junction depletion region, and hence the tunnel barriers: at $V_{SG1} = V_{SG2} = -70$ mV, the potential from the splitgates is shallow, giving a wide depletion region and a current of 0.5 nA for the first electron Coulomb peak at $V_{SD} = 10$ mV. At $V_{SG1} = V_{SG2} = -270$ mV, the potential across the p-n junction is steeper, now giving a narrower depletion region and a current of 13 nA for the first electron. (The $V_{SG1/2} = -270$ mV trace has been offset in V_{BG} and in current.).

To overcome these limitations, we have developed a new method of integrating multiple local gates with ultraclean fabrication. A schematic of the device is shown in Fig. 1. As described in the Methods, we grew a carbon nanotube over gates that were patterned in a thin doped silicon layer. Our current design provides three independent gates, although fabrication can easily be modified to include a scalable number of gates inside the trench (see Supplementary Information). In this Letter, we use these three gates in two different ways. In device D1, with $L = 1.5$ μm, the gates are used to define a single-electron and single-hole quantum dot where electrons and holes are confined by tunable p–n junctions instead of Schottky contacts. In device D2, with $L = 300$ nm, we rely on tunnel barriers from the Schottky contacts, but now use the three gates to create a tunable single-electron and single-hole double quantum dot.

In all previous measurements of quantum dots in carbon nanotubes containing a single electron, carriers were confined by Schottky barriers formed at the metal contacts[9,17], or by potentials defined from trapped oxide charges[18]. In Fig. 2 we demonstrate a single-electron quantum dot defined only by gate voltages. We begin by applying a negative voltage to the splitgates, creating a p-type nanotube source and drain on top of the oxide. Sweeping the backgate voltage V_{BG}, shown in Fig. 2a, the current initially shows weak modulations from resonances in the leads when the suspended segment is p-type (ppp configuration), and is then completely suppressed as the suspended segment is depleted (pip configuration). As we sweep further, we form a pnp quantum dot showing clean Coulomb blockade, where single electrons in the suspended segment are confined by p–n junctions to the leads. Figure 2c shows a stability diagram as a function of both backgate and bias voltage, demonstrating that we have reached the single-electron regime. As the confinement potential and doping profile are determined by our local gates, we can also confine single holes

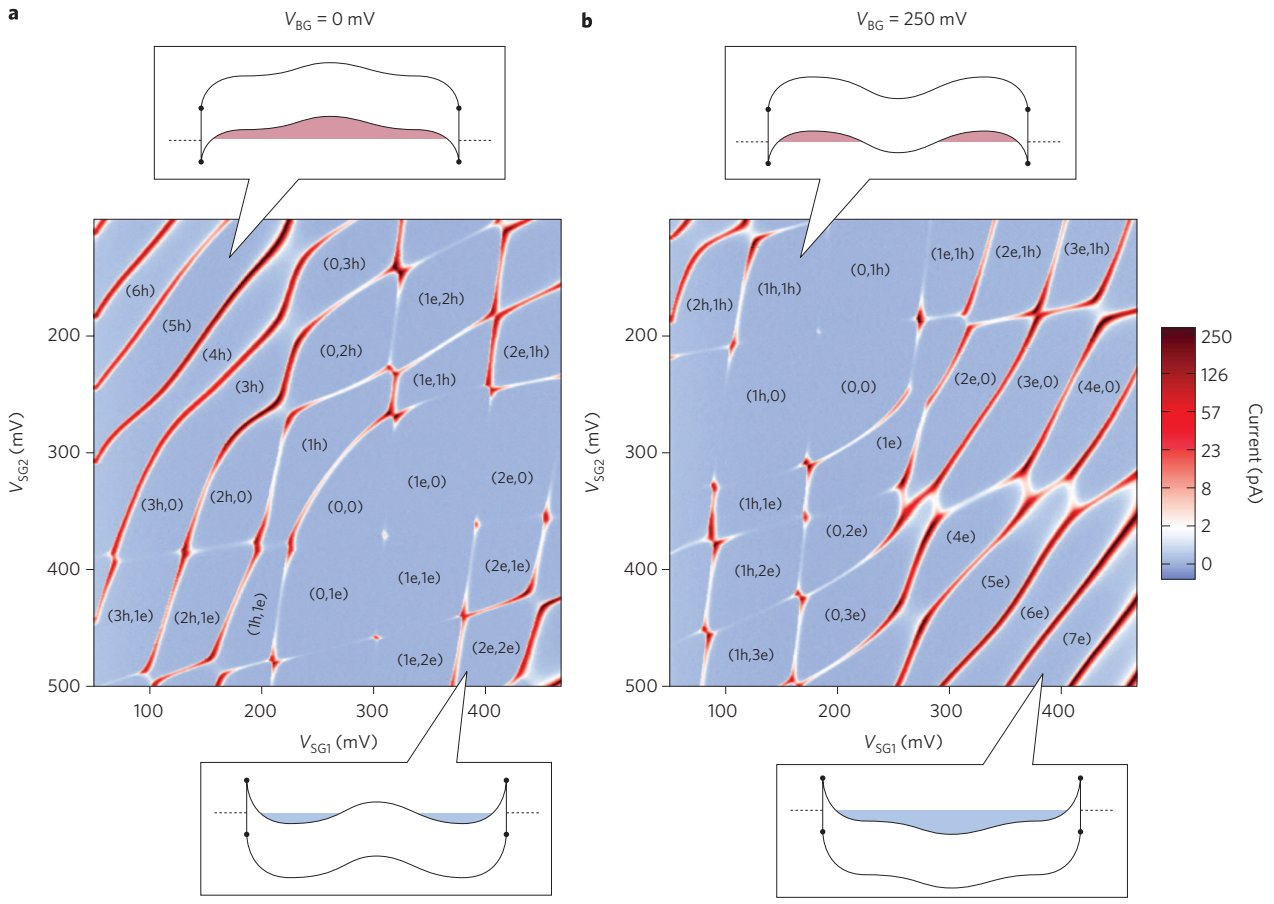

Figure 3 | A tunable double quantum dot in the few-electron and few-hole regime. Current as a function of the two splitgate voltages at $V_{SD} = 0.5$ mV for device D2. In device D2, electrons are confined in the nanotube by Schottky barriers at the metal contacts, with a potential that is tunable using the three gates. Electron and hole occupation numbers are determined from the transition to a pn double quantum dot, as described in the Supplementary Information. **a**, $V_{BG} = 0$. At this voltage, a barrier for electrons is induced in the middle of the device. Electrons are added to a weakly coupled double dot potential, and holes are added to a single dot potential. **b**, $V_{BG} = 250$ mV. A more positive V_{BG} creates a double dot potential for holes and a single dot potential for electrons. The interdot coupling for both the electron and the hole double dot can be tuned continuously using the backgate voltage.

in an npn configuration in the same device simply by inverting the gate voltages, shown in Fig. 2d. In Fig. 2e we show the current as a function of the backgate voltage and the voltage on the splitgates. In the left of the plot, the leads are doped p-type, and a positive backgate induces a single-electron pnp quantum dot. In the right of the plot, the leads are doped n-type and a negative backgate induces a single hole npn quantum dot. By adjusting the splitgate voltages, the p–n junction width, and thus the tunnel barriers, can be tuned while keeping the electron number fixed (see Fig. 2f).

In device D2, we use the gates in our design for a different purpose. We rely on less transparent Schottky contacts as incoming and outgoing tunnelling barriers, and now use the backgate and the two splitgates as three independent local gates to create a double quantum dot potential in the nanotube with a tunable interdot coupling. Figure 3 shows the current through the device as a function of the two splitgate voltages. In the lower left and upper right regions of the plots, the two splitgates dope the two segments of the nanotube with carriers of opposite sign, resulting in a pn double quantum dot with an interdot barrier formed from a p–n junction. In the upper left (bottom right) corner, the two splitgates dope both sides of the nanotube p-type (n-type). In Fig. 3a, V_{BG} is set to ground, which gives a potential in the middle of the nanotube that is attractive for holes but repulsive for electrons. We consequently observe single dot behaviour for the first hole and weakly coupled double dot behaviour for the first electron. In Fig. 3b, we apply a positive backgate voltage, $V_{BG} = 250$ mV. The potential in the middle of the nanotube is now repulsive for holes; the first hole enters a weakly coupled double dot, and electrons fill a mostly single dot potential. (At some gate voltages, the presence of the oxide creates a non-uniform potential that results in strongly coupled double dot instead of purely single dot behaviour. See Supplementary Section S1.) By changing V_{BG}, we can continuously tune the interdot coupling in the few-electron and few-hole regime from weakly coupled double dot to single dot behaviour.

In Fig. 4, we investigate the tunable inderdot coupling in our double quantum dot in more detail by studying current at the (0,1e)↔(1e,0) triple point transition of a weakly coupled double quantum dot. In a weakly coupled double quantum dot, current can only flow at specific values of the gate voltages, known as triple points, where the levels in the two dots are aligned, allowing an electron to tunnel from one dot to the other[21]. In Fig 4a to c, V_{BG} is made more negative, creating a larger barrier for electron tunnelling between the dots, suppressing the current at the triple point. However, as we sweep V_{BG} further, (Fig. 4d, e), the current increases again, despite creating an even larger barrier for electron tunnelling.

The explanation of this curious increase of the current is a novel tunnelling process analogous to the tunnelling paradox in high-energy physics proposed by Klein[14–16]. Specifically, we will define Klein tunnelling as any enhancement of the tunnelling of an electron through a barrier due to the so-called negative energy solutions

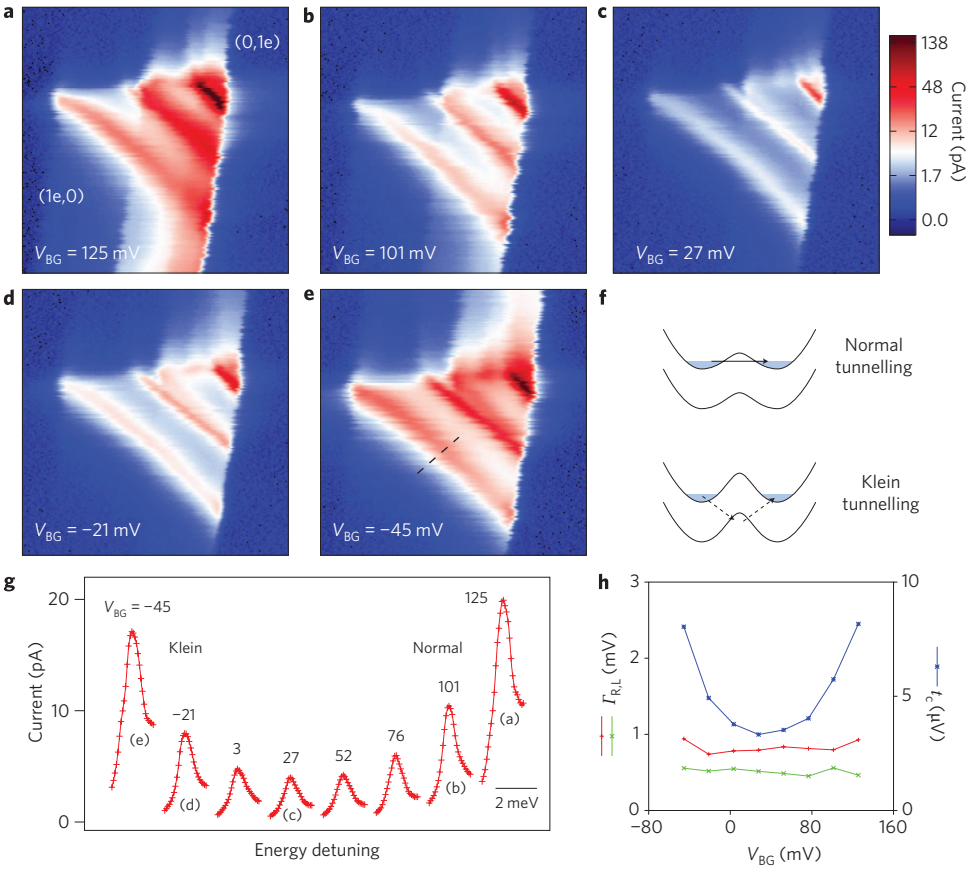

Figure 4 | Klein tunnelling in a single-electron double quantum dot. Current at the (0,1e) ↔ (1e,0) triple point for a single electron double quantum dot at $V_{SD} = 5$ mV. (Note that the interdot capacitance $E_c^{inter} \approx 0.2$ mV is much smaller than the bias, and thus the triple point bias triangles for the electron and hole cycle[21] strongly overlap.) Transitions to the excited state of the outgoing dot are visible as lines in the triangle running parallel to the baseline and give a quantized level spacing of 3 mV, consistent with a dot length of ~500 nm. **a–c**, The backgate is made more negative, creating a larger barrier for electron tunnelling. As a result, the current through the double dot is decreased. **d, e**, The current begins to increase again despite a larger barrier for electron tunnelling. **f**, This increase in current results from tunnelling of an electron below the barrier through a virtual state in the valence band, analogous to Klein tunnelling in high-energy physics. **g**, Line cuts of the triple point data in **a–e** showing the current for the ground-state baseline transition at different backgate voltages. The line cuts are taken along the dashed line in **e**. The *x* axis shows the distance along this line converted into the energy detuning between the left and right dot ground-state levels. For the rightmost traces, interdot tunnel coupling is mediated by normal electron tunnelling, and for the leftmost traces, Klein processes provide the interdot tunnel coupling. **h**, Parameters from a fit to the Stoof–Nazarov equation. The interdot tunnel coupling initially decreases as the barrier height increases ($V_{BG} = 125$ to 27 mV), and then increases due to the onset of Klein tunnelling as the barrier height becomes comparable to the bandgap ($V_{BG} = 27$ to −45 mV).

(positron states) that arise in relativistic quantum mechanics (see Supplementary Information for further discussion). In Fig. 4, the enhancement of the interdot coupling we observe at large tunnel barrier heights is an example of Klein tunnelling in a carbon nanotube, where the valence band of the nanotube now plays the role of the negative energy solutions in relativistic quantum mechanics. What is unique about the data in Fig. 4 is that we have created a direct implementation of Klein's gedanken experiment in our double quantum dot device, where we are able to tune continuously from the normal tunnelling regime to the Klein tunnelling regime simply by changing the barrier height with a gate voltage. We have also observed Klein tunnelling for holes (see Supplementary Information). In Fig. 4, what we observe is a kind of 'virtual' Klein tunnelling, where the electron virtually occupies a state in the empty valence band in order to tunnel from the left to the right dot, similar to a cotunnelling process[22]. In addition to our observations in a double quantum dot, the npn data in Fig. 2 can be thought of as a type of Klein tunnelling in a different regime, where the valence band is now occupied with holes, and where Klein tunnelling occurs by the electron sequentially tunnelling across the two p–n junctions. This also emphasizes the close relation between Klein tunnelling in high-energy physics and interband tunnelling phenomena in semiconductor physics, such as Zener tunnelling in insulators[23] and direct interband tunnelling in an Esaki diode[24].

Analysing the current at the (0,1e) ↔ (1e,0) transition quantitatively using the result from Stoof and Nazarov[25,26], we calculate the tunnel rates Γ_L and Γ_R of the barriers to the leads, and the interdot tunnel coupling t_c, shown in Fig. 4h. At these gate voltages, we are in the limit of weak interdot coupling: $t_c \approx 5\ \mu V \ll \Gamma_L, \Gamma_R \approx 0.6$ mV. The interdot coupling t_c is decreased from an initial value of 9 μV to a minimum of 3 μV as a function of backgate voltage, before the onset of Klein tunnelling results in an increase up to 9 μV as we approach gate voltages where an npn triple dot is formed. Γ_L and Γ_R are found to be independent of the backgate voltage, indicating that the backgate is not influencing the Schottky barrier transparency.

Finally, note that although we are in the appropriate double quantum dot coupling regime, we have not found evidence of spin blockade at any of the expected transitions[27]. (A parallel magnetic field of 1.5 T was applied to ensure that the nanotube valley degeneracy was lifted). One possible explanation for this is a singlet–triplet

splitting in the (0,2e) state that is much smaller than the 3 mV single particle spacing we observe in the single-electron quantum dot. This could be an indication of the formation of a Wigner crystal[20], in which the electron wavefunction overlap is very small, and consequently the single–triplet splitting is strongly suppressed. This possibility will be investigated further using devices with more gates, which could allow us to probe the Wigner crystallization transition by tuning the quantum dot confinement potential.

We have presented a new technique for confining single electrons and single holes in ultraclean carbon nanotubes. By eliminating disorder and incorporating local gates, a new level of control over single-electron confinement has been achieved, allowing us to observe a novel type of tunnelling in a single-electron carbon nanotube device. Although our motivation for such a device comes from the spin physics of carbon nanotubes[28], the fabrication itself could have a much broader use. This may include electrically doped p–n junctions for carbon nanotube optical emission[29], where low disorder and multiple gates for electrical control of p–n junctions could allow the development of new types of optically active devices.

Methods

Fabrication began with a p^{++} silicon wafer with 285 nm of thermal silicon oxide. On top of this, a 50-nm-thick n^{++} polysilicon gate layer was deposited, followed by a 200-nm LPCVD–TEOS oxide layer. Using electron-beam lithography and dry etching, a trench ~300 nm deep was etched, forming the two splitgates from the n^{++} silicon gate layer. A 5/25 nm W/Pt layer was deposited to serve as source and drain contacts, and nanotubes were then grown from patterned Mo/Fe catalyst[30]. In about half of the devices, a single carbon nanotube was suspended across the trench making electrical contact to the source and drain. Transport through the devices was characterized at room temperature, and selected devices were cooled to $<$300 mK for low temperature transport measurements. In total, we measured 11 devices at low temperatures, of which 4 reached the single electron regime. Here we present data from two small bandgap devices: D1 with $L = 1.5$ μm, $W = 300$ nm and bandgap $E_g = 60$ mV, and D2 with $L = 300$ nm, $W = 500$ nm and $E_g = 25$ mV, where bandgaps were determined by subtracting the charging energy from the size of the empty dot Coulomb diamond.

Received 29 September 2008; accepted 23 February 2009; published online 6 April 2009

References

1. Hanson, R., Kouwenhoven, L. P., Petta, J. R., Tarucha, S. & Vandersypen, L. M. K. Spins in few-electron quantum dots. *Rev. Mod. Phys.* **79,** 1217–1266 (2007).
2. Mason, N., Biercuk, M. J. & Marcus, C. M. Local gate control of a carbon nanotube double quantum dot. *Science* **303,** 655–658 (2004).
3. Sapmaz, S., Meyer, C., Beliczynski, P., Jarillo-Herrero, P. & Kouwenhoven, L. P. Excited state spectroscopy in carbon nanotube double quantum dots. *Nano Lett.* **6,** 1350–1355 (2006).
4. Jørgensen, H. I., Rasmussen, G. K., Hauptmann, J. R. & Lindelof, P. E. Single wall carbon nanotube double quantum dot. *Appl. Phys. Lett.* **89,** 232113 (2006).
5. Gräber, M. R. *et al.* Molecular states in carbon nanotube double quantum dots. *Phys. Rev. B* **74,** 075427 (2006).
6. Loss, D. & Divincenzo, D. P. Quantum computation with quantum dots. *Phys. Rev. A* **57,** 120–126 (1998).
7. Petta, J. R. *et al.* Coherent manipulation of coupled electron spins in semiconductor quantum dots. *Science* **309,** 2180–2184 (2005).
8. Koppens, F. H. L. *et al.* Universal phase shift and nonexponential decay of driven single-spin oscillations. *Phys. Rev. Lett.* **99,** 106803 (2007).
9. Kuemmeth, F., Ilani, S., Ralph, D. C. & McEuen, P. L. Coupling of spin and orbital motion of electrons in carbon nanotubes. *Nature* **452,** 448–452 (2008).
10. Nowack, K. C., Koppens, F. H. L., Nazarov, Y. & Vandersypen, L. M. K. Coherent control of a single electron spin with electric fields. *Science* **318,** 1430–1433 (2007).
11. Bulaev, D. V., Trauzettel, B. & Loss, D. Spin-orbit interaction and anomalous spin relaxation in carbon nanotube quantum dots. *Phys. Rev. B* **77,** 235301 (2008).
12. Fujisawa, T., Austing, D. G., Tokura, Y., Hirayama, Y. & Tarucha, S. Allowed and forbidden transitions in artificial hydrogen and helium atoms. *Nature* **419,** 278–281 (2002).
13. Elzerman, J. M. *et al.* Single-shot read-out of an individual-electron spin in a quantum dot. *Nature* **430,** 431–435 (2004).
14. Klein, O. Die Reflexion von Elektronen an einem Potentialsprung nach der relativistischen Dynamik von Dirac. *Z. Phys.* **53,** 157–165 (1929).
15. Katsnelson, M. I., Novoselov, K. S. & Geim, A. K. Chiral tunnelling and the Klein paradox in graphene. *Nature Phys.* **2,** 620–625 (2006).
16. Trauzettel, B., Bulaev, D. V., Loss, D. & Burkard, G. Spin qubits in graphene quantum dots. *Nature Phys.* **3,** 192–196 (2007).
17. Jarillo-Herrero, P., Sapmaz, S., Dekker, C., Kouwenhoven, L. P. & van der Zant, H. S. Electron–hole symmetry in a semiconducting carbon nanotube quantum dot. *Nature* **429,** 389–392 (2004).
18. Minot, E. D., Yaish, Y., Sazonova, V. & Mceuen, P. L. Determination of electron orbital magnetic moments in carbon nanotubes. *Nature* **428,** 536–539 (2004).
19. Cao, J., Wang, Q. & Dai, H. Electron transport in very clean, as-grown suspended carbon nanotubes. *Nature Mater.* **4,** 745–749 (2005).
20. Deshpande, V. V. & Bockrath, M. The one-dimensional Wigner crystal in carbon nanotubes. *Nature Phys.* **4,** 314–318 (2008).
21. van der Wiel, W. G. *et al.* Electron transport through double quantum dots. *Rev. Mod. Phys.* **75,** 1–22 (2002).
22. De Franceschi, S. *et al.* Electron cotunneling in a semiconductor quantum dot. *Phys. Rev. Lett.* **86,** 878–881 (2001).
23. Zener, C. A theory of the electrical breakdown of solid dielectrics. *Roy. Soc. Proc.* **145,** 523–529 (1934).
24. Esaki, L. New phenomenon in narrow germanium p–n junctions. *Phys. Rev.* **109,** 603–604 (1958).
25. Stoof, T. H. & Nazarov, Y. Time-dependent resonant tunneling via two discrete states. *Phys. Rev. B* **53,** 1050–1053 (1996).
26. Fujisawa, T. *et al.* Spontaneous emission spectrum in double quantum dot devices. *Science* **282,** 932–935 (1998).
27. Ono, K., Austing, D. G., Tokura, Y. & Tarucha, S. Current rectification by Pauli exclusion in a weakly coupled double quantum dot system. *Science* **297,** 1313–1317 (2002).
28. Churchill, H. O. H. *et al.* Electron–nuclear interaction in ^{13}C nanotube double quantum dots. Preprint at <http://arxiv.org/abs/0811.3236>.
29. Misewich, J. A. *et al.* Electrically induced optical emission from a carbon nanotube FET. *Science* **300,** 783–786 (2003).
30. Kong, J., Soh, H. T., Cassell, A. M., Quate, C. F. & Dai, H. Synthesis of individual single-walled carbon nanotubes on patterned silicon wafers. *Nature* **395,** 878–881 (1998).

Acknowledgements

It is a pleasure to acknowledge P.L. McEuen for the suggestion of using p–n junctions as tunable barriers, as well as D. Loss, T. Balder, I.T. Vink, R.N. Schouten, L.M.K. Vandersypen, and M.H.M. van Weert for useful discussions and suggestions. This research was supported by the Dutch Organization for Fundamental Research on Matter (FOM), the Netherlands Organization for Scientific Research (NWO), and the Japan Science and Technology Agency International Cooperative Research Project (JST-ICORP).

Author contributions

G.A.S. was responsible for the experimental work. All authors discussed the results and commented on the manuscript.

Additional information

Supplementary information accompanies this paper at www.nature.com/naturenanotechnology. Reprints and permission information is available online at http://npg.nature.com/reprintsandpermissions/. Correspondence and requests for materials should be addressed to G.A.S.